

Numerical and Experimental Investigation of Three-Dimensional Hydrodynamic Focusing in Polydimethylsiloxane (PDMS) Microchannels

Chih-Chang Chang, Zhi-Xiong Huang and Ruey-Jen Yang

Department of Engineering Science, National Cheng Kung University,
Tainan, Taiwan, 70101, rjyang@mail.ncku.edu.tw

ABSTRACT

In this work, we have designed and fabricated a three-dimensional hydrodynamic focusing microfluidic device. The device comprises two-layer PDMS microchannels structure. Sample flow stream was firstly vertically constrained into a narrow core-region, and then horizontally focused into one small window from cross-section perspective, which is useful for cell/particle counting. We have show the numerical and experimental images of the focused stream shape from cross-section perspective, experimental ones were captured using confocal fluorescence microscope. We have also investigated the effect of channel aspect ratio on vertical focusing effect using CFD simulations. The results show that the sample flow can be focused successfully in lower aspect ratio (~ 0.5) of main channel in our design. Furthermore, the effect of Reynolds number on the vertical focusing effect was also investigated. The numerical results show that the rectangular-like shape of the focused stream from cross-section perspective was deformed as Reynolds number is high due to stronger secondary flows was produced in vertical focusing element. This phenomenon was also demonstrated experimentally. In other words, the chip only works well at low Reynolds number (< 5). The device can be integrated into on-chip flow cytometry.

Keywords: microfluidics, hydrodynamic focusing, flow cytometry

1 INTRODUCTION

Manipulating fluid flow in microchannels is a highly important issue in the design of microfluidic systems. Hydrodynamic focusing technique [1] provides an effective means of controlling the passage of chemical reagent or bio-samples through microfluidic channels. The conventional two-dimensional hydrodynamic focusing approach in planar micro-devices involving using two neighboring sheath flows to constrain the central sample flow laterally (horizontally) within the center of the microchannel. This approach provides the ability to position small volume of analytes precisely in two dimensions to the region of detection. Recently, two-dimensional hydrodynamic focusing has been successfully demonstrated in a wide variety of microfluidic applications, including in micro-flow cytometers for cell/particle

counting and sorting [2], rapid diffusion-based micro-mixers for the kinetic studies of protein folding [3,4] etc. Achieving a precise control of the focused stream width is crucial in various applications. A more general theoretical model has been proposed by our current research group [5], which is capable of predicting the focused stream width as a function of the relative sheath and sample flow rates for rectangular microchannels with various aspect ratios.

The application of two-dimensional hydrodynamic focusing in cell/particle counting in planar micro-flow cytometers, the cells or particles may not pass the focused stream one by one even though the focused stream width is focused to the same order of magnitude of as that of the cell size. This is because they may be located at different depths of microchannel as their size is smaller than channel height. There are two approaches to solve this issue in planar micro-devices. One is three-dimensional dielectrophoretic (DEP) force focusing [6, 7] or combined two-dimensional hydrodynamic focusing and DEP force [8], another is three-dimensional hydrodynamic focusing [9-10]. They offer the advantages of positioning of cells/particles in both vertical and horizontal dimensions. It can avoid them locating at different depths and is more suitable for optical detection. The current study is focused on the design and fabrication of three-dimensional hydrodynamic focusing device.

An ideal three-dimensional hydrodynamic focusing would be achieved by completely surrounding the sample flow by a cylindrical sheath flow that constrains it to the center of the channel. It can be easily achieved by using a co-jet device consists of two capillary tubes with different diameters. In practice, this device is difficult to fabricate using planar micro-fabrication processes. In recent years, some three-dimensional complicated structures for three-dimensional hydrodynamic focusing have been proposed using conventional micro-fabrication methodologies [9, 10]. In this work, we present a simple structure for three-dimensional hydrodynamic focusing shown in Figure 1, which comprises two-layer PDMS microchannels. This structure is similar to that of Ref. [11]. The difference between them is the geometry of vertical focusing element. The vertical focusing units of Ref.[11] and the current study are shown in Figure 2 (a) and (b), respectively. They are named "DESIGN I" and "DESIGN II" in this study. This study also presents a numerical comparison of them. The sample flow in this device is constrained using multiple sheath flows, as shown in Figure 1 (b) and (c). The sample flow (B stream) is firstly constrained vertically to a narrow stream by two sheath flows (A and C stream), and then

horizontally focused into a small window from cross-section perspective (see Figure 1(d)) by additional sheath flows (D stream) from the sides as in two-dimensional hydrodynamic focusing. The three-dimensional hydrodynamic focusing effect in this device is demonstrated both numerically and experimentally.

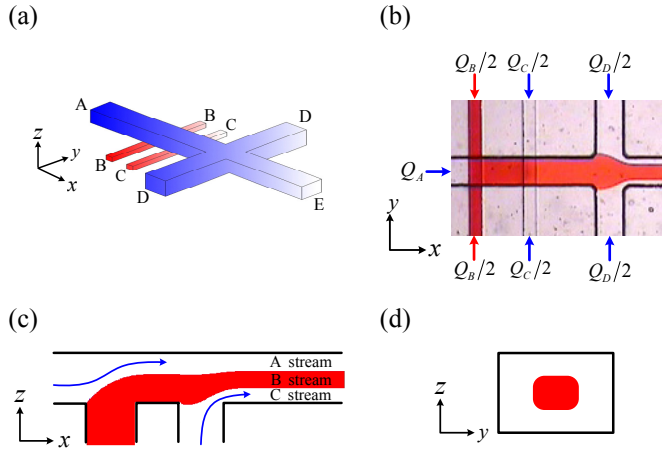


Figure 1: Schematic illustration of the three-dimensional hydrodynamic focusing device. (a) 3-D view, (b) top view, (c) side view, and (d) cross-section perspective.

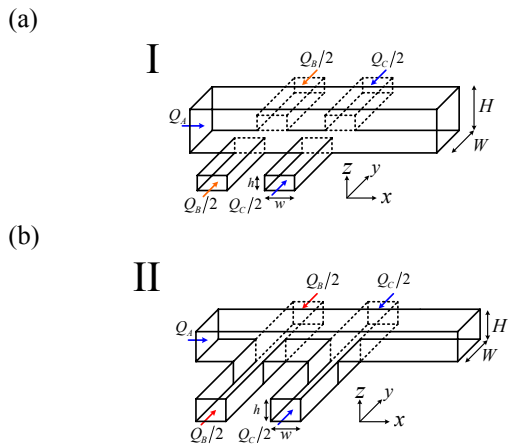


Figure 2: The geometry of vertical focusing element. (a) design of Ref.[11], and (b) design of our work.

2 EXPERIMENTAL SECTION

2.1 Fabrication of Microfluidic Chip

The three-dimensional hydrodynamic focusing device of the current study was fabricated using well-known PDMS micromolding techniques [12]. The device consists of two-layer PDMS structures, one is top layer and another is bottom layer. For the formation of the PDMS microchannel structures of top and bottom layers, two master molds were firstly formed onto a silicon wafer by using a negative

photoresist SU-8 layer (MicroChem Corp, MA, USA). The thickness of the photoresist layer was controlled by the spin rate. Following soft baking, standard lithography procedures were performed to form the microchannel structures. After fabricating SU-8 master molds, PDMS precursor poured onto the master mold and then cured at a temperature 65°C for 1h. The inverse structures of SU-8 master mold were then transferred onto the PDMS microchannels after the de-molding process. Finally, the chip was assembled by sealing the two PDMS layers together using an oxygen plasma treatment. A photograph of the assembled microfluidic chip is shown in Figure 3. The dimensions of the chip were measured to be 4 cm in width and 7 cm in length. The size of the microchannels of top layer is $100\mu\text{m}$ in width and $95\mu\text{m}$ in height (channel “A”, “D” and “E”), and that of bottom layer is $50\mu\text{m}$ in width and $45\mu\text{m}$ in height (channel “B” and “C”).

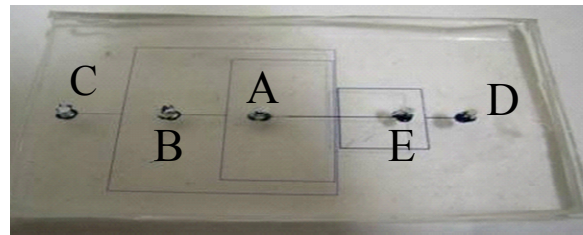


Figure 3: Photographs of microfluidic chip capable of three-dimensional hydrodynamic focusing.

2.2 Experimental Setup

The three-dimensional hydrodynamic focusing experiments were performed using deionized water for the sheath flows from A, C, and D inlet ports and deionized water mixed with red dye or Rhodamine B for the sample flow from B inlet port. The deionized water for the sheath and sample flows were stored in four 10 ml plastic syringes and then driven through the device by two syringe pumps (Scientific Inc., model KD 200 series, USA). The current study deliberately adopted the syringe pumps to drive the fluids since it permitted the volumetric flow rates of the sheath and sample flows to be precisely controlled. Images of the hydrodynamic focusing effect from top view were acquired using an optical microscope (Nikon, model TE300, Melville, NY, USA) integrated with a CCD camera (CFMDIO, model TE/CCD512TKM, Taiwan). Furthermore, the cross-sectional images of the sample focused streams were taken with a laser scanning confocal fluorescence microscope (Leica TCS MP II).

3 GOVERNING EQUATIONS AND NUMERICAL METHODS

The steady state flows in the three-dimensional hydrodynamic focusing device are governed by continuity

and momentum equations. Sample (or dye) transport in microchannels can be described by the species convection-diffusion equation. The current study adopts the artificial compressibility method to solve the continuity and momentum equations together with their corresponding boundary conditions. These equations are discretized using finite difference method and then solved using an approximate factorization method.

4 RESULTS AND DISCUSSION

4.1 Influence of Channel Aspect Ratio on Vertical Focusing Effect

In this section, we present a numerical comparison of the vertical focusing units of DESIGN I and DESIGN II in the aspect of main channel (center channel) aspect ratio. In Figure 4, it indicates that the sample flow cannot be constrained successfully in lower aspect ratio channel in the case of DESIGN I, $H/W = 0.6$ especially, even though the height of side channels h is much smaller than that of main channel H . The sample flow only vertically focused into a rectangular-like shape stream successfully and perfectly in the case of high aspect ratio $H/W = 6.0$. This is the reason that the main channel of vertical focusing unit in Ref.[11] is designed to high aspect ratio (approximately 6.6). Note that Reynolds number is defined as $Re = UD_h/\nu$, U is the average velocity in the downstream of vertical focusing element $U = (Q_A + Q_B + Q_C)/(H \times W)$ (note: $Q_A = Q_C$ in this study) and the hydraulic diameter $D_h = 2(H \times W)/(H + W)$. The flow rate ratio of sheath flow to sample flows of vertical focusing is defined as $\alpha_v = 2Q_A/Q_B$. By contrast, from Figure 5, it can be seen that the sample flow can be constrained successfully in vertical dimension in the main channel with lower aspect ratio in DESIGN II even if $H/W = 0.5$.

4.2 Influence of Reynolds Number on Vertical Focusing Effect in DESIGN II

In vertical focusing unit, the sample flow (B stream) and sheath flow (C stream) flow from the channels of bottom layer, the z -direction flow velocity exists in the main channel, the secondary flows in the vertical focusing element may be induced as the total flow rate of sample and sheath flow is increased. The secondary flows will result in the non-ideal focused stream shape. Thus, the flow conditions in vertical focusing element should be considered. From Figure 6, it can be seen clearly that the magnitude of secondary flow increases as the Reynolds number is increased due to the stronger inertial force, the rectangular-like shape of the focused stream only is maintained at lower Reynolds number. This phenomenon is also demonstrated experimentally, as shown in Figure 7. It

can be seen clearly that the focused stream is twisted seriously as the Reynolds number is 100. In our CFD simulations, the appropriate operating condition is $Re < 5$. Similarly, the shape of the focused stream in DESIGN II is also deformed by the secondary flow as the Reynolds number is high.

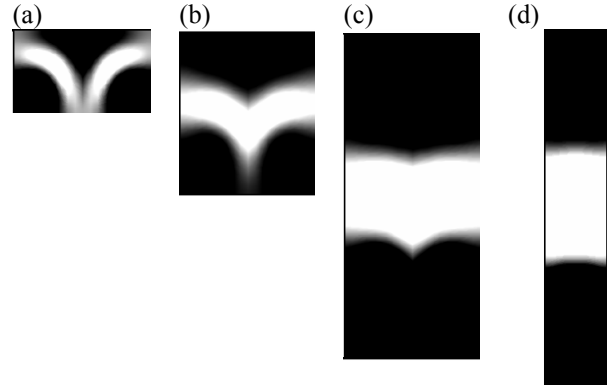


Figure 4: Numerical images of the cross-sectional profiles of vertical focused stream in the main channel of DESIGN I with different aspect ratios, (a) $H/W = 0.6$, (b) $H/W = 1.2$, (c) $H/W = 2.4$, and (d) $H/W = 6.0$. Note that the ratio $h/H = 12$, flow rate ratio $\alpha_v = 1.0$ and $Re = 1.0$.

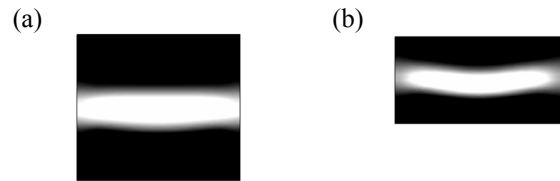


Figure 5: Numerical images of the cross-sectional profiles of vertical focused stream in the main channel of DESIGN II with different aspect ratios (a) $H/W = 0.95$, (b) $H/W = 0.5$. Note that $\alpha_v = 1.0$ and $Re = 1.0$.

4.3 Confocal Fluorescence Microscope Images of Three-Dimensional Focused Sample Stream

Figure 8 shows that the cross-sectional profiles of the focused stream after the vertical and horizontal focusing processes. The experimental images are captured using confocal fluorescence microscope. Here the flow rate ratio of the horizontal focusing is defined as $\alpha_h = (Q_D)/(2Q_A + Q_B)$. In both numerical and experimental images, it can be seen clearly that the sample flow is successfully focused into a small rectangular-like window for different flow rate ratios. The numerical and experimental results are consistent in qualitative comparison.

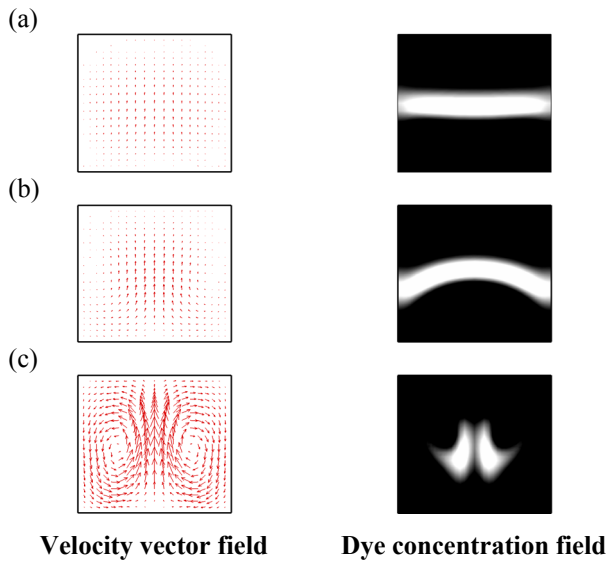


Figure 6: Secondary flow fields and shapes of vertically focused stream from cross-section perspective in the main channel. (a) $Re = 1.0$, (b) $Re = 10$, and (c) $Re = 100$. Note that $H/W = 0.95$ and $\alpha_v = 2.0$, the flow fields were plotted near the channel “C”, and the concentration fields were plotted in the downstream of vertical focusing element.

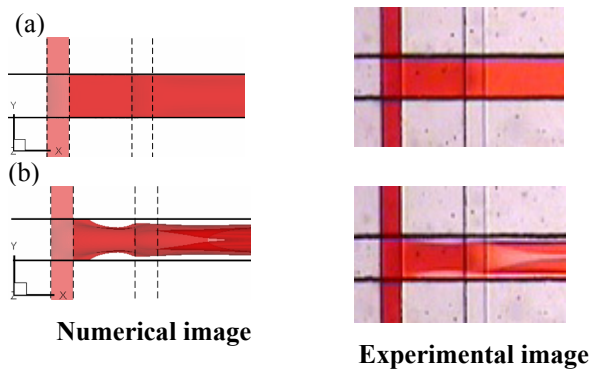


Figure 7: Comparison of numerical and experimental images from top view for different Reynolds numbers (a) $Re = 1.0$, and (b) $Re = 100$. Here $\alpha_v = 1.0$.

5 CONCLUSIONS

In the present study, a three-dimensional hydrodynamic focusing device comprises two-layer PDMS microchannels substrate has been proposed. Sample flow stream in this device can be focused successfully into a small core-region after the vertical and horizontal focusing processes, which is more suitable for cell/particle counting compared to the conventional two-dimensional hydrodynamic focusing. The results have also shown that the vertical focusing can be achieved in the smaller aspect ratio of main channel (approximately 0.5) relative to the design in Ref.[11]. The rectangular-like shape of the focused stream in the vertical

focusing element was deformed when Reynolds number was increased. This is because the stronger secondary flow was induced. Therefore, the focusing device only works well at low Reynolds number regime (approximately less than 5). Under the appropriate operating conditions, this device can be integrated into on-chip flow cytometry for cell or particle counting.

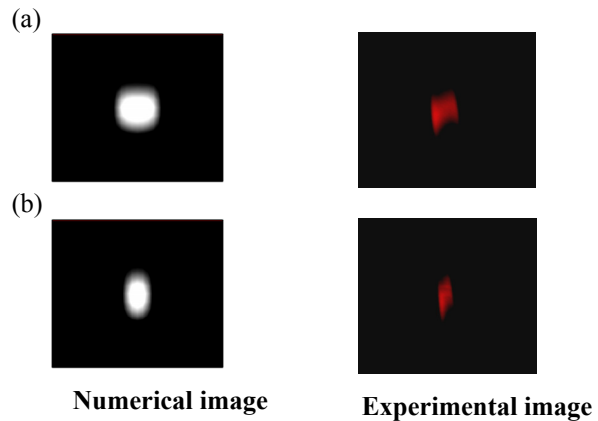


Figure 8: Images of the focused stream in the downstream of the main channel for different focusing ratios, (a) $\alpha_v = 0.0$, $\alpha_h = 1.0$, (b) $\alpha_v = 1.0$, $\alpha_h = 1.0$, (c) $\alpha_v = 1.0$, $\alpha_h = 2.0$. Note that Re is approximately 1.7 and $H/W = 0.95$.

REFERENCES

- [1] P. Crosland-Taylor, *Nature*, 17, 37-38, 1953.
- [2] D. Huh, W. Gu, Y. Kamotani, J. B. Grotberg and S. Takayama, *Physiol. Meas.*, 26, R73-98, 2005.
- [3] J. B. Knight, A. Vishwanath, J. P. Brody and R. H. Austin, *Phys. Rev. Lett.*, 80, 3863-3866, 1998.
- [4] D. E. Hertzog, X. Michalet, M. Jager, X. Kong, J. G. Santiago, S. Weiss and O. Bakajin, *Anal. Chem.*, 76, 7169-7178, 2004.
- [5] G.-B. Lee, C.-C. Chang, S.-B. Huang and R.-J. Yang, *J. Micromech. Microeng.*, 16, 1024-1032, 2006.
- [6] C. Yu, J. Vykoukal, D. M. Vykoukal, J. A. Schwartz, L. Shi and P. R. C. Gascoyne, *J. Microelectromech. Syst.*, 14, 481-487, 2005.
- [7] H. Morgan, D. Holmes and N. G. Green, *IEE Proc. Nanobiotechnol.*, 150, 76-81, 2003
- [8] D. Holmes, H. Morgan and N. G. Green, *Biosens. Bioelectron.*, 21, 1621-1630, 2006.
- [9] N. Sundararajan, M. S. Pio, L. P. Lee and A. A. Berlin, *J. Microelectromech. Syst.*, 13, 559-567, 2004.
- [10] R. Yang, D. L. Feedback and W. Wang, *Sens. Actuators A*, 113, 71-77, 2005.
- [11] C. Simonnet and A. Groisman, *Appl. Phys. Lett.*, 87, 114104, 2005.
- [12] D. C. Duffy, J. C. McDonald, O. J. A. Schueller and G. M. Whitesides, *Anal. Chem.*, 70, 4974-4984, 1998.